American Journal of Pathology, Vol. 157, No. 2, August 2000

Liver Damage using Suicide Genes

A Model for Oval Cell Activation

Matilde Bustos,* Bruno Sangro,* Pilar Alzuguren,* Ana Gloria Gil,* Juan Ruiz,* Naiara Beraza,* Chen Qian,* Angeles Garcia-Pardo,† and Jesus Prieto*

From the Division of Hepatology and Gene Therapy, Clinica Universitaria and Medical School, University of Navarra, Pamplona; and the Centro de Investigaciones Biologicas,† CSIC, Madrid, Spain*

Liver regeneration from the facultative hepatic stem cells, the oval cells, takes place in situations in which liver regeneration from pre-existing hepatocytes is prevented. Different models have been used to stimulate oval cell response. Many of them involve the use of carcinogenic agents with or without partial hepatectomy. In this study we show that adenovirus-mediated gene transfer of the suicide gene thymidine kinase followed by ganciclovir administration caused hepatotoxicity of variable intensity. Rats with moderate elevation in serum transaminases recovered normal liver architecture few weeks after adenovirus injection. In contrast, rats with severe liver damage exhibited a marked and persisting activation of oval cells accompanied by ductular hyperplasia. In some rats, such lesion eventually evolved to cholangiofibrosis and in one rat to cholangiocarcinoma. Deposition of fibronectin and increased number of hepatic stellate cells were found in association with oval cells and cholangiofibrotic lesions. Hepatocyte growth factor was hyperexpressed in the livers with intense oval cell response or ductular proliferation, suggesting a participation of this factor in those lesions. In summary, our data demonstrate activation of oval cell response after gene transfer of thymidine kinase followed by ganciclovir administration. These findings indicate that high doses of this therapy causes liver damage together with an impairment in hepatocellular regeneration. ***(Am J Pathol 2000, 157:549–559)***

It has been postulated that there is a liver-committed stem cell compartment that does not take part in normal tissue renewal but does proliferate in response to certain forms of liver injury.[1,2] Oval cells are considered to be the progeny of activated hepatic stem cells, a belief supported by the fact that this particular cell type expresses markers thought to be characteristic of stem cells.[3] The principle supported by studies in animal models of liver injury is that oval cells participate in the restoration of the functional liver mass after hepatic damage when the noxious agent reduces the number of viable liver cells but the ability of the surviving hepatocytes to regenerate is either totally nullified or at least severely impaired. Experimental models to activate the oval cell compartment include the performance of 2/3 hepatectomy on rats treated with acetyl-aminofluorene (AAF),[4] the administration of dipin to mice,[5] and of furan to rats.[6] Oval cell proliferation has also been shown in rats treated with galactosamine and in Long-Evans Cinnamon rats which have a defect in the *ATP7B* gene resulting in toxic accumulation of copper in the liver.[7,8] Proliferation of oval cells also takes place in $p21^{CIP1/WAF1}$ transgenic mice when overexpression of the transgene is directed to the liver.[9] Stem cells are considered to be a possible target for carcinogenic agents, since their longevity permits the development of the multistep process leading to tumor formation along the prolonged latency period between exposure and progression to cancer.[10] However, the role of oval cells in the pathogenesis of primary tumors in the liver is still unresolved.

During past years, the approach based on the transfer of so-called suicide genes to tumor cells has emerged as a promising strategy in cancer gene therapy.[11] A commonly used suicide gene is herpes simplex virus (HSV) thymidine kinase (tk) which confers sensitivity to ganciclovir (GCV). HSV-tk transforms GCV into a phosphorylated derivative with potent cytotoxic activity. In a previous study we reported that intraportal injection of an adenoviral vector expressing HSV-tk (AdCMVtk) followed by GCV administration resulted in marked reduction of the tumor mass in an animal model of multifocal hepatocellular carcinoma, but this antitumoral effect was accompanied by high mortality due to severe hepatotoxicity.[12] Although early toxic liver changes have been described after gene therapy with AdCMVtk plus GCV,[13] the long term follow up of animals subjected to this treatment has not been previously reported. The present study was undertaken to characterize the evolution of the

Supported by the Comision Interministerial de Ciencia y Tecnologia, Spain, SAF 96–0268.

Accepted for publication May 19, 2000.

Address reprint requests to Matilde Bustos, Division of Hepatology, School of Medicine, University of Navarra, Pamplona, 31008, Spain. E-mail: mbustos@unav.es.

liver damage which occurs in rats after intravascular injection of AdCMVtk followed by GCV administration. Our results show that this treatment causes hepatotoxicity and stimulates oval cell proliferation. In animals with moderate hepatocellular damage activation of oval cells was inconspicuous and liver architecture was normal few weeks after injection of the adenovirus. However, in cases with more intense liver cell damage a marked proliferation of oval cells was found during the first 6 weeks. This reaction was followed by nodular regeneration and marked ductular proliferation. Some animals developed intestinal metaplasia and cholangiofibrosis. Cholangiocarcinoma was found in one rat sacrificed at week 36. Our data show that the AdCMVtk/GCV system is a useful model to activate the oval cell compartment, to explore the pathophysiology of the liver stem cells and to study the pathological changes which result from disturbances in oval cell differentiation. Furthermore, our data emphasize the need to adjust the dose of the adenoviral vector when considering treatment of liver neoplasms using suicide genes to avoid undue toxicity.

Materials and Methods

Male Wistar rats (250 to 290 g) were obtained from Harlan Interfauna Iberica, S.A. (Barcelona, Spain). OV-6, BD1, BD2 monoclonal antibodies were gifts from Dr. Douglas Hixson (Brown University, Providence, RI). Proliferating cell nuclear antigen (PCNA) and α-smooth muscle actin antibodies were from Dako A/S (Copenhagen, Denmark). Monoclonal antibody against desmin was from Sigma Chemical Company (St. Louis, MO). Anti-fibronectin was provided by Dr Angeles Garcia (CSIC, Madrid, Spain). Polyclonal antibodies against TGF-β, HGF, and c-met were purchased from Santa Cruz Biotechnology, Inc. (Santa Cruz, CA). HGF cDNA was a gift from Dr. Jiro Fujimoto (University of Hyogo, Nishinomiya, Japan). Anti-mouse immunoglobulin labeled with peroxidase or with fluorescein isothiocyanate (FITC) and anti-rabbit immunoglobulin labeled with FITC and 3,3′-diaminobenzidine tetrahydrochloride were from Sigma. Ganciclovir (Cymevene) was purchased from Roche S.A. (Madrid, Spain) and incorporated into time-released ALZET osmotic pumps supplied by Criffa S.A. (Barcelona, Spain).

Adenoviral Vectors

The recombinant adenoviral vectors AdCMVtk and AdCMVlacZ expressing the HSV-tk gene and the reporter gene lacZ under the control of the cytomegalovirus enhancer/promoter (CMV) were constructed as previously described.[11] These vectors were expanded in 293 cells and purified by double cesium chloride ultracentrifugation. The purified virus was extensively dialyzed against 10 mmol/L Tris per 1 mmol/L of $MgCl_2$ and stored in aliquots at −80°C. The virus titer was determined by spectrophotometry and plaque assay as described.[11]

Treatment Protocol

Young adult male Wistar rats weighing 250 to 290 g were in cages maintained at room temperature under a 12-hour light/dark illumination cycle in an approved biohazard animal room. Standard pelleted chow and drinking water were administered *ad libitum* throughout the entire experimental protocol. All of the animal experimentation described in this study was conducted according to institutionally approved protocol.

The rats were divided into two groups: 53 in the experimental group and 27 in the control group. Each rat in the experimental group received 2 ml of suspension containing 4×10^{10} pfu/kg of AdCMVtk which was slowly injected into the tail vein. At this moment an osmotic pump (2ML2 ALZET) with GCV solution was placed intraperitoneally to deliver the drug at the dose of 30 mg/kg/day for 14 days. Control rats received 2 ml of phosphate-buffered saline (PBS) into the vein tail and PBS was also placed into the pump. After 14 days the pumps were removed and checked for complete emptying.

Rats from the experimental and control group were sacrificed under ether anesthesia at 1, 2, 3, 4, 5, 6, 7, 8, and 36 weeks after the administration of the adenoviral vector or PBS (Table 1). To test the adenovirus-mediated gene transfer efficiency to liver cells, a group of 6 rats were given an intravenous injection of AdCMVlacZ at the same those as AdCMVtk. After 48 hours, livers were removed and 5-bromo-4-chloro-3-indolyl-β-D-galactoside staining (X-gal) was used to detect lacZ gene expression as previously described.[11]

Histology, Histochemistry, Immunohistochemistry, and Biochemistry

Liver tissue was removed at each time point as indicated above and was divided and fixed in either 10% buffered neutral formalin or placed in OCT compound, frozen in cold 2-metylbutane (Merck, Darmstadt, Germany) and stored at −80°C. All of the staining procedures for light microscopy were performed on 4-μm-thick, paraffin-embedded sections or on 6-μm-thick, frozen sections. Routine histological examinations were made for all liver tissue samples on sections (paraffin and frozen) stained with hematoxylin-eosin. Histochemical demonstration of glucose-6-phosphatase (G6Pase) activity was performed according to the method of Wachstein and Meisel.[14]

Immunohistochemical staining was carried out in frozen tissue with monoclonal antibodies against OV6, BD1, BD2, and desmin using as a second antibody anti-mouse immunoglobulin labeled with peroxidase. The chromogenic reaction was developed with diaminobenzidine. Fibronectin immunoreactivity was detected with anti-rabbit immunoglobulin labeled with FITC. Detection of PCNA, α-smooth muscle, HGF, c-met and TFG-β was performed after heating formalin-fixed paraffin-embedded tissue sections by ~800-W microwaving in 0.01 mol/L citric acid buffer pH 6.0, followed by incubation with the corresponding antibody and anti-mouse (PCNA and α-smooth muscle actin) or anti-rabbit (HGF, c-met,

Table 1. Histology of Liver Biopsies

Weeks after administration of adenoviral vector	No. of rats	Relevant findings
1	6	Infiltration of mononuclear cells at the periportal areas
2	6	Ductular proliferation of different intensity at the portal tracts
3	4	Infiltration of the hepatic lobule by oval cells irradiating from the portal tracts
	1	Few oval cells in some portal tracts
	1	Normal liver architecture
4	2	Massive infiltration and proliferation of oval cells
	2	Few oval cells in a few portal tracts
	2	Normal liver architecture
5–6	6	Abundant oval cells and nodules of small hepatocytes at the portal tracts
	2	Few oval cells in a few portal tracts
	6	Normal liver architecture
	2	Nodular pattern of hepatocellular regeneration and proliferating ductules
7	4	Normal liver architecture
	1	Proliferating bile ducts with intestinal metaplasia
8	3	Ductular proliferation with intense fibrosis and intestinal metaplasia
	2	Normal liver architecture
36	1	Cholangiocarcinoma
	2	Normal liver architecture

and TFG-β) immunoglobulin labeled with peroxidase. For each antibody, negative controls were performed by omitting the primary antibody from the protocol. Negative control sections were included with c-met (SP260) antibody that had been neutralized by pretreatment with the immunizing peptide sc-162P (Santa Cruz).

Aspartate aminotransferase (AST) levels were determined in serum by automatic calorimetric assays (Technicon RA-1000, Bayer).

Western Blot Analysis of c-met Protein Expression

Frozen liver tissue was homogenized in RIPA buffer (9.1 mmol/L Na_2HPO_4, 1.7 mmol/L NaH_2PO_4, 150 mmol/L NaCl, 1.0% Nonidet P-40, and 0.1% sodium dodecyl sulfate (SDS), 0.05% sodium deoxycholate, and 1.1 mmol/L phenylmethylsulfonyl fluoride) with protease inhibitor cocktail tablets (Boehringer Mannheim, Mannheim, Germany). The protein content was determined by the Bradford assay (Bio-Rad, München, Germany). A total of 30 μg of protein was dissolved in the sample buffer heated at 90°C for 5 minutes and analyzed by 7.5% SDS-polyacrylamide gel electrophoresis. Immunoreactivity was visualized by incubation with Supersignal CL-HRP chemiluminescence substrate (Pierce Chemical, Rockford, IL).

Northern Blot

Total RNAs were isolated by a modified acid/guanidine thiocyanate/phenol/chloroform method[15] using ULTRASPEC (Biotecx Laboratories, Inc, Houston, TX) reagents according to the manufacturer's instructions. RNA concentrations were determined spectrophotometrically.

For Northern blotting total RNA (20 μg) was electrophoresed under denaturing conditions, transferred onto nylon membranes positively charged (Boehringer Mannheim), and fixed by UV cross-linking. The quality and comparative quantity was estimated on gels by ethidium bromide staining. The 2.6 kb rat HGF cDNA and the cDNA probe for β-actin was labeled by random priming (Amersham Pharmacia Biotech Inc. Buckinghamshire, UK) and used for Northern blot. Membranes were prehybridized for 1 hour and hybridized 2 hours with QuikHyb (Stratagene, La Jolla, CA) at 68°C. The membranes were stringently washed and exposed to Kodak XAR film.

In Situ *Hybridization*

The rat albumin cDNA used for *in situ* hybridization (ISH) corresponds to 700 bp fragment from the 3′ end of the rat albumin gene cloned into $pGEM_1$. After linearizing the vector with *Hin*dIII or *Eco*RI, a digoxygenin-labeled antisense and sense cRNA probe were synthesized with T7 or SP6 RNA polymerase (BRL, Gibco) respectively using the DIG RNA labeling kit (Boehringer Mannheim) according to manufacturer's instructions. The cRNA probes were purified by ethanol precipitation and correct size verified by 1.5% agarose gel electrophoresis. Typical yields of 10 μg of DIG-labeled cRNA for 1 μg of DNA were obtained.

ISH was performed on paraffin-embedded tissue sections. After deparaffinization and rehydration, sections were immersed in 0.2% Triton/PBS pH 7, followed by incubation with proteinase K (80 μg/ml) for 30 minutes at 37°C. They were then acetylated in triethanolamine containing 0.25% acetic anhydride. The sections were hybridized in buffer containing 0.01 mol/L Tris/HCl, pH 7.5, 12.5% Denhardt's solution (0.02% Ficoll, 0.02% bovine serum albumin, 0.02% polyvinylpyrrolidone), 2X SSC, 50% formamide, 0.5% SDS, 250 μg/ml salmon sperm DNA, 5 mg/ml sodium pyrophosphate, and the cRNA probe for 18 hours at 45°C. The following day, the sections were washed twice in 2X SSC/0.1% SDS for 10 minutes at room temperature, twice in 0.1X SSC/0.1% SDS at 43°C, and then treated with RNase A at 37°C for 15 minutes. Immunological detection of albumin mRNA was performed by reaction with anti-DIG antibody coupled to alkaline phosphatase using nitroblue tetrazolium and 5-bromo-4-chloro-3-indolphosphate in a dark box for

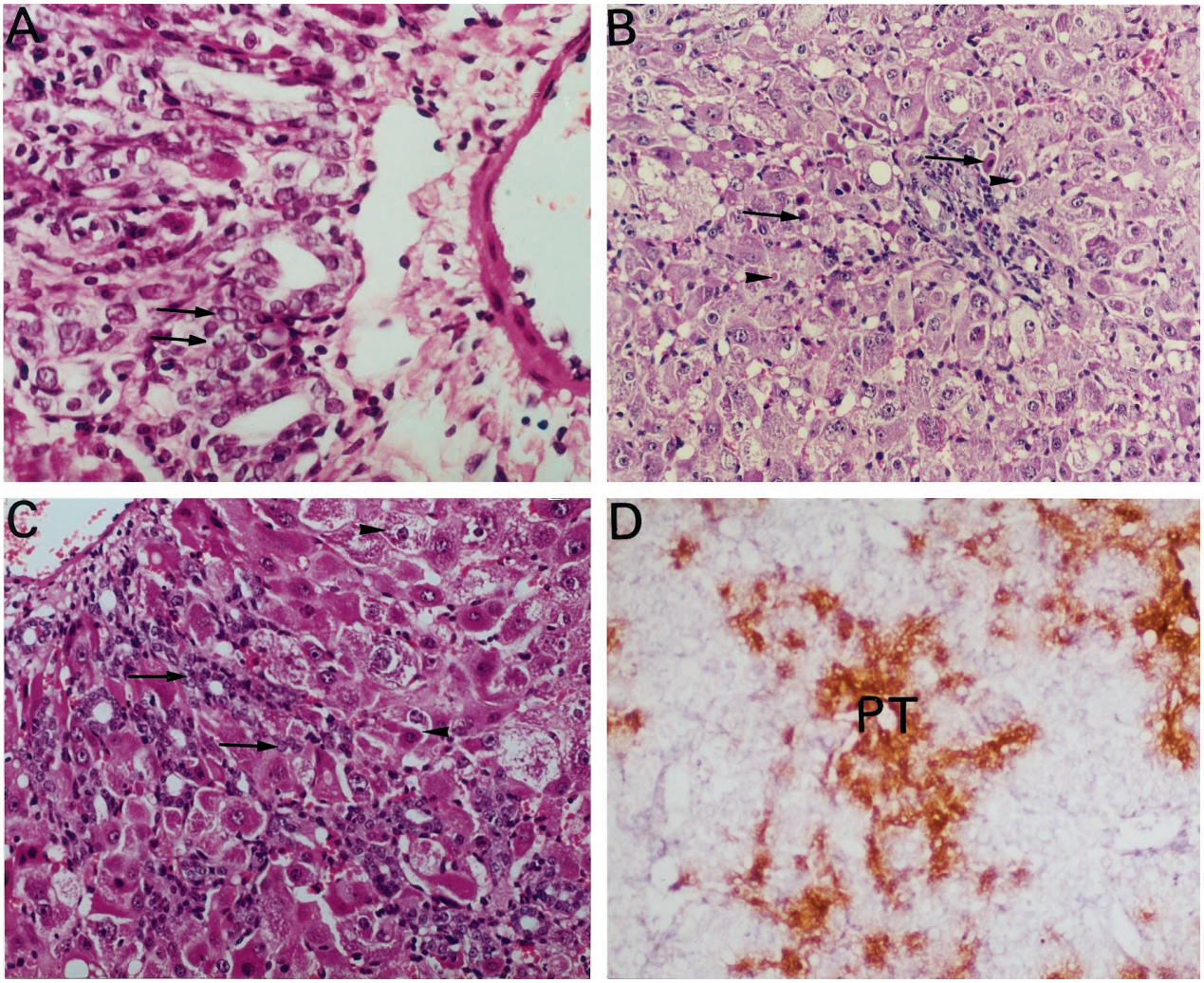

Figure 1. Liver sections obtained from rats at weeks 2 and 4 after administration of AdCMVtk plus ganciclovir. **A:** After 2 weeks, periportal region shows marked proliferation of ductular formations and small oval cells (**arrows**) with ovoid nucleus and peripheral heterochromatin penetrating into the hepatic lobule (H&E, ×400). **B:** Histopathological changes in the liver showing cellular damage with the presence of acidophilic bodies (**arrows**), apoptotic bodies (**arrowheads**) and swelling of hepatocytes resulting in paleness and foamy appearance of the cytoplasm (H&E, ×200). **C:** At week 4, the liver showed marked proliferation of oval cells (**arrows**) invading densely the hepatic lobule from the portal tracts. These cells penetrate as cords and ductular formations between hepatocytes. Ballooning degeneration and acidophilic hepatocytes are observed (**arrowheads**) (×200). **D:** BD2 immunohistochemical staining of liver sections at the fourth week. Intense staining of proliferating oval cells which fan out from the portal tract (PT) inside the hepatic lobule (×100).

2 hours, after which the color reaction was stopped with TE buffer and the slides were mounted in glycerol/PBS. Negative controls included hybridization with the sense probe and omission of the RNA probe or anti-DIG antibody.

Statistical Analysis

Mann-Whitney *U* tests were used to compare variables between two groups. A value of $P < 0.05$ was considered significant.

Results

Histology

After intravenous injection of AdCMVlacZ, about 75% of hepatocytes stained positively with X-gal. There was, however, a total absence of transduction of bile duct epithelial cells (data not shown). No staining was found in organs other than the liver except a faint signal in renal proximal tubules in one of the rats tested.

Rats which received AdCMVtk followed by GCV treatment suffered a chain of morphological changes in the liver which are summarized in Table 1. As shown in this table, groups of 6 animals were sacrificed at weeks 1, 2, 3, 4, 7, and 8. Fourteen rats were sacrificed at weeks 5 and 6 and three at week 36. A moderate infiltration of mononuclear cells in the portal tract was observed on the first week after administration of the adenovirus. On the second week, in four of the six rats studied there were abundant acidophilic bodies and apoptotic bodies (Figure 1A) indicating severe hepatocellular damage. In these rats a ductular proliferation was apparent in the vicinity of the limiting plate where small oval cells forming duct-like structures were identified (Figure 1B). These

cells reacted positively with OV-6 and BD2, two monoclonal antibodies directed against rat oval cell markers.[16]

On the third week after administration of AdCMVtk, signs of liver cell damage and a conspicuous dysplasia of hepatocytes together with the presence of oval cells in the portal tracts which tended to infiltrate the hepatic lobules was observed in 4 animals. In two other animals both hepatocellular damage and oval cell reaction were less noticeable. On the fourth week, two rats exhibited signs of severe liver cell injury with swelling and ballooning degeneration of hepatocytes accompanied by a massive proliferation of oval cells which invaded the hepatic lobule radiating from the portal spaces along the plates of hepatocytes (Figure 1, C and D). These small epithelial cells which stained positively for BD2 and OV-6, were disposed as rows or clusters and frequently formed ductular structures (Figure 1, C and D). Proliferating oval cells showed positive PCNA staining. Two rats of this group showed less liver damage with few oval cells at the portal tracts. A normal liver architecture was observed in two more rats (Table 1).

On weeks 5 and 6, six rats showed massive substitution of the liver tissue by proliferating small OV-6 and BD2 positive cells (Figure 2A) which diffusely infiltrated the cords of damaged and dysplastic hepatocytes. In two rats, oval cell proliferation was much less intense and in six animals liver architecture was normal. As shown in Figure 2B, in animals with marked activation of the stem cell compartment it was possible to observe nodules of basophilic hepatocytes which showed a round nuclei and scant cytoplasm and were frequently surrounded by small OV-6 and BD2 positive cells (Figure 2C) which stained positively for PCNA. Whereas oval cells lacked G6Pase activity, this enzymatic activity was present in the nodules of small hepatocytes (Figure 2D) although at levels considerably lower than those observed in hepatocytes of a normal liver (data not shown). We also analyzed by *in situ* hybridization the expression of albumin mRNA as an additional marker of hepatocellular differentiation. We observed that the levels of albumin transcripts were low in the old damaged hepatocytes while both oval cells and the nodules of small basophilic hepatocytes showed strong albumin mRNA expression (Figure 2E). Thus, the presence in these nodules of an intense albumin signal (as in oval cells) and a G6Pase activity which is intermediate between OV-6 positive cells (absent G6Pase) and mature normal hepatocytes (high G6Pase activity) strongly suggests that the small basophilic hepatocytes represent newly formed liver cells which derive from oval cells and replace old damaged hepatocytes at the portal areas.

Interestingly, animals which developed marked proliferation of oval cell at 3, 4, 5, and 6 weeks after the administration of adenovirus, showed at the time of sacrifice higher serum levels of aspartate-aminotransferase (869 $\pm$ 239.3 UI/ml) than rats with small (135.6 $\pm$ 45.9; $P < 0.01$) or absent oval cell reaction (and 83.00 $\pm$ 10.5; $P < 0.01$ *versus* cases with intense oval cell proliferation).

On week 7, two rats showed a nodular pattern of hepatocellular regeneration and persistence of proliferating ductules with positive oval cell markers at the edge of the nodules (Figure 2F). The rest of the rats presented normal liver architecture. Similarly, four of six rats sacrificed at week 8 showed nodular hepatocytic regeneration with abundant OV-6 and BD2 positive ductular formations surrounding the nodules (Figure 3A). These hyperplastic ductules showed positive PCNA staining indicating proliferative activity of the epithelial cells (Figure 3B). At this time point most of the bile ductular cells of such lesions also stained positively with BD1, an antibody which recognizes mature bile duct epithelium.[17] In one of these rats, proliferating bile ducts were supported by a thin fibrotic stroma and some of the ductules were filled with mucus and exhibited intestinal metaplasia and goblet cells. In three rats, ductular proliferation was more intense and periductular fibrosis was more prominent (Figure 3C). Some of the glandular structures in these cholangiofibrotic lesions exhibited also intestinal metaplasia with the presence of enterocyte differentiation and goblet cells (Figure 3D). Expression of HGF was detected by immunohistochemistry only in metaplastic glands (Figure 3E). Immunohistochemical expression of the HGF receptor, c-met, was found in metaplastic glands and dysplastic bile epithelium of proliferating ductules (Figure 3F). Expression of c-met was less intense in non-dysplastic proliferating ductules. These data were confirmed by Western blot that demonstrated a 140-kd band which was more pronounced in the liver from rats with cholangiofibrosis or with ductular proliferation and intestinal metaplasia than in normal liver (Figure 4). A cholangiocarcinoma with glands which displayed positivity for both c-met and PCNA was found in one of the three rats sacrificed at week 36.

Interestingly, animals which developed nodular transformation and ductular hyperplasia or cholangiofibrosis at weeks 7 or 8 after the administration of the adenovirus showed at the time of sacrifice higher serum levels of aspartate-aminotransferase (342.66 $\pm$ 113 UI/ml) than rats with normal liver architecture (113 $\pm$ 19 UI/ml) ($P < 0.05$).

Role of Hepatic Stellate Cells and Growth Factors in Proliferation of Oval Cells

In livers showing proliferation of oval cells irradiating from the portal area into the hepatic lobule, we observed that the proliferating cells were surrounded by fibronectin deposition (Figure 5A). Intermingled with this extracellular matrix component, there were many desmin positive cells, indicating a participation of HSC in this modality of liver cell regeneration (Figure 5B). HSC showed positivity for α-smooth muscle actin, especially in cholangiofibrotic lesions found on the 8th week after AdCMVtk administration (Figure 5C). In these lesions abundant fibronectin deposition and TGF-β were found surrounding the proliferating bile ducts (Figure 5, D and E).

It has been reported that HGF is expressed by sinusoidal lining cells in close vicinity to proliferating oval cells in other experimental designs.[20] This factor appears to play an important role in all aspects of stem cell behavior including proliferation, migration and differentia-

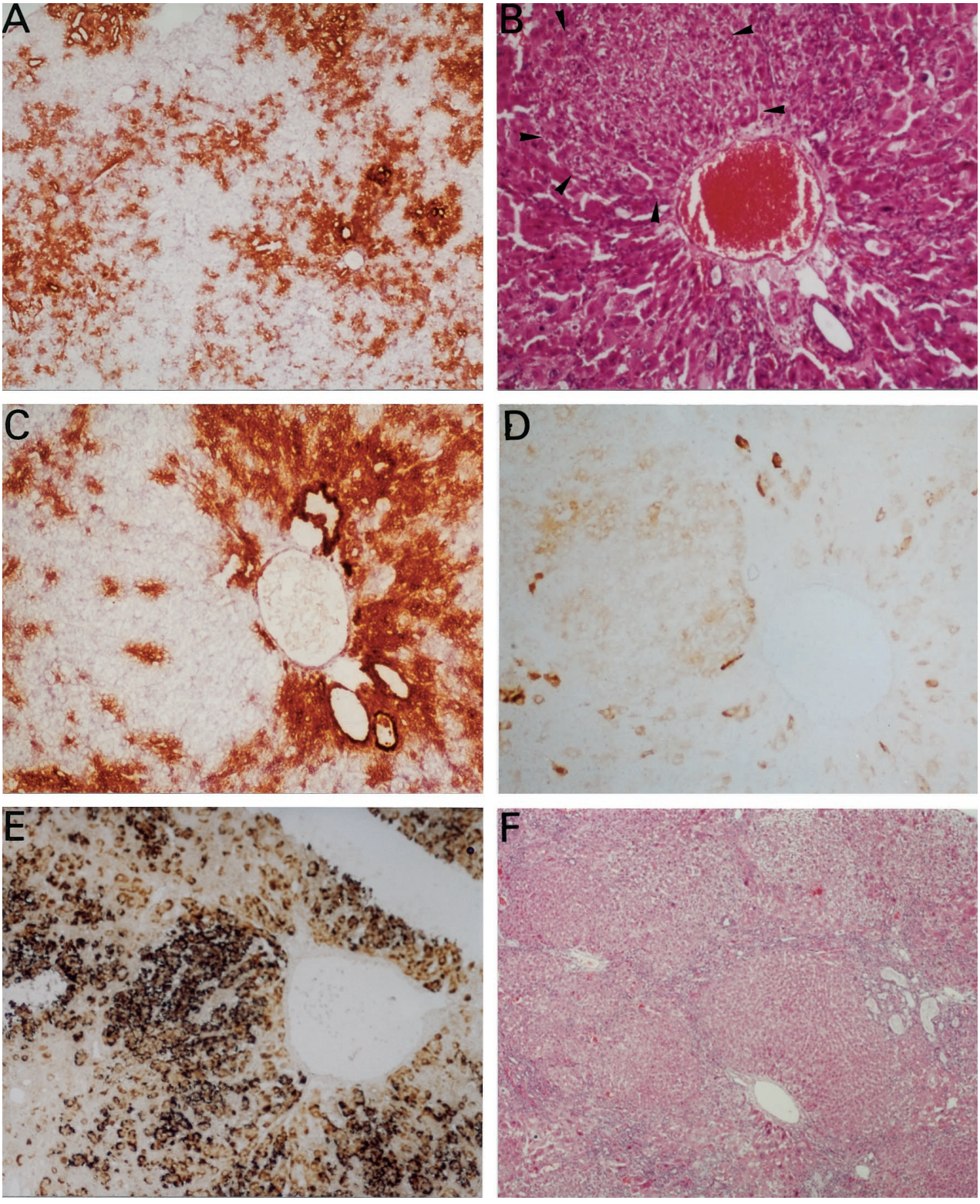

Figure 2. Liver sections obtained at weeks 6 and 7 after administration of AdCMVtk plus ganciclovir. **A:** BD2 immunohistochemical staining of proliferating oval cells 6 weeks after administration of adenovirus. The liver parenchyma has been replaced by ductular structures which are decorated with anti-BD2 (×40). **B:** **Arrows** indicate a nodule of small hepatocytes which appear to replace the dysplastic and swollen hepatocytes of the damaged liver at week 6 (H&E, ×200). **C:** Immunohistochemical staining for BD2 showing positivity of oval cells around the portal tract while the new and small hepatocytes are negative for this marker (×200). **D:** Histochemical staining of glucose-6-phosphatase in the same liver specimen, showing low activity of the enzyme in the nodule of small hepatocytes (×200). **E:** *In situ* hybridization for albumin mRNA showing a strong positivity in the nodule of new hepatocytes and positivity in the oval cells close to the portal tracts in contrast with the low signal in old damaged hepatocytes. **F:** Seven weeks after administration of AdCMVtk one rat showed nodular regeneration and proliferation of oval cells at the edge of the nodules (H&E, ×40).

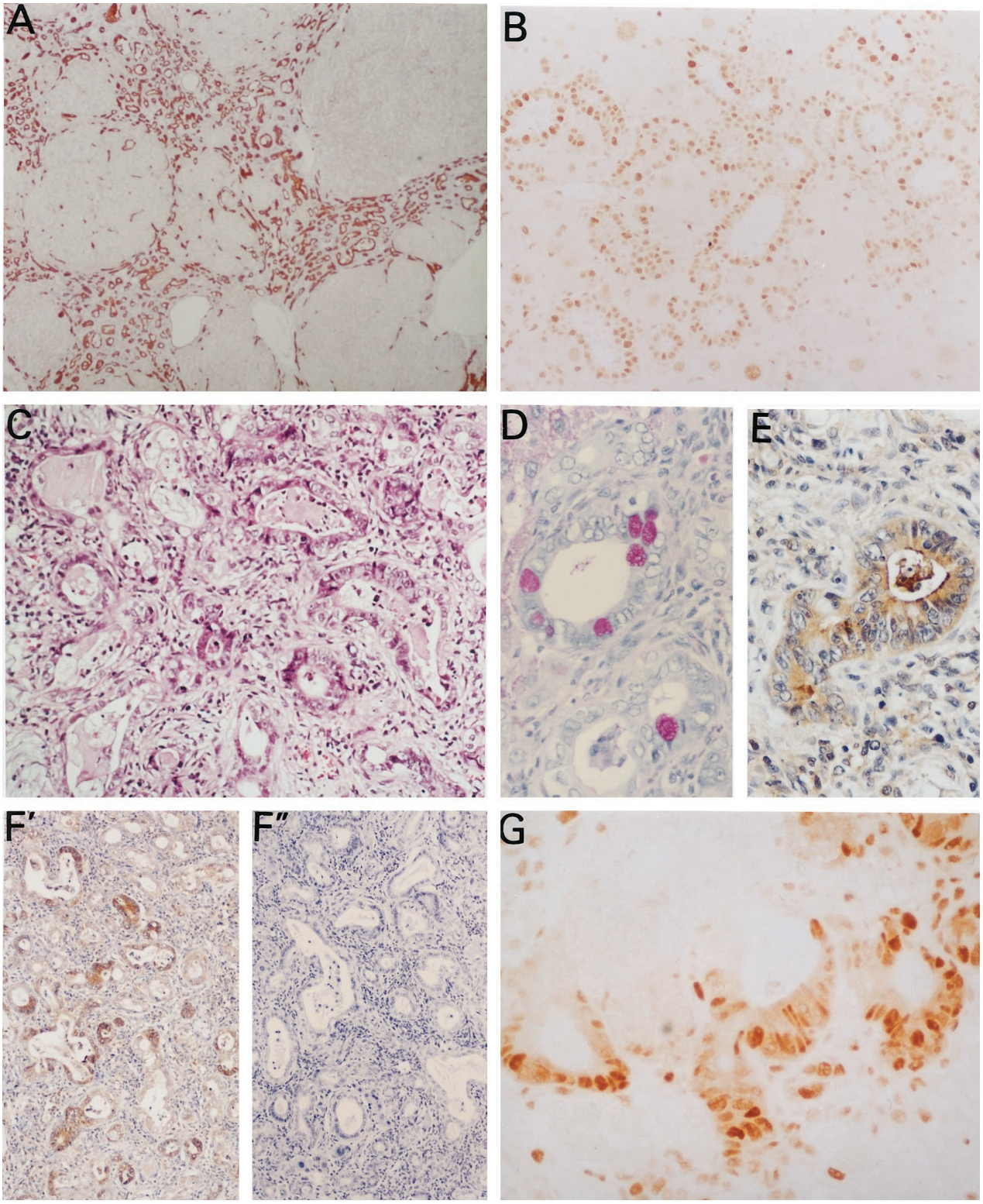

Figure 3. Light micrographs at 8 weeks after administration of adenoviral vector. **A:** Section of the liver from one rat showing nodular regeneration with marked bile ductular hyperplasia exhibiting OV-6 positivity (×40). **B:** PCNA immunostaining of proliferating ductules (×200). **C:** Cholangiofibrosis at week 8 with marked dysplasia, hyperchromasia and presence of mitosis in dysplasic glands (H&E, ×200). **D:** Intestinal metaplastic glands with enterocyte-like and goblet cells (PAS, ×400). **E:** Intestinal metaplastic glands showing immunoreactivity for HGF (×400). **F′:** Immunohistochemical staining of c-met showing strong expression of this protein in intestinal metaplastic glands and weaker in biliary ductular formations. **F″:** Negative control of c-met immunohistochemistry after incubation of the anti c-met antibody with the immunizing peptide. **G:** PCNA immunostaining in the cholangiofibrotic lesion of the same specimen demonstrating intense positivity in dysplastic ductular structures (×400).

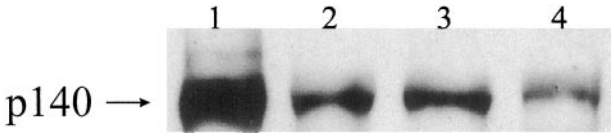

Figure 4. Representative Western blot of c-met protein. As a positive control[1] an established human biliary adenocarcinoma cell line (SK-Cha1) (kindly provided by Strazzabosco) was used. As shown in the figure a strong immunoreactive band at 140 kd and a faint band at 170 kd (possibly an immature precursor of c-met) was observed in SK-Chal cell line. In cases with intestinal metaplasia associated with cholangiofibrosis[2] or with proliferating bile ducts[3] one band at 140 kd was observed. This band was weaker in normal rat liver.[4]

tion.[21] Thus, we have analyzed by Northern blot the expression of HGF in the liver in our model. As shown in Figure 6, HGF mRNA was not detected in normal liver. However, we found very high levels of HGF mRNA in the liver at weeks 1 and 2 after administration of adenovirus by Northern Blot. The amount of HGF transcripts decreased slightly by week 3 but increased on subsequent weeks although only in animals with persistent oval cell proliferation. In cholangiofibrosis HGF mRNA expression was present but at levels which were lower than in cases with high number of proliferating oval cells.

Discussion

The use of suicide genes has been proposed as an attractive modality of cancer gene therapy. The most commonly used suicide gene is HSV-tk which transforms GCV into a triphosphorylated derivative. This compound blocks DNA synthesis and although it is especially toxic for dividing cells, it can also cause damage of non-dividing epithelial cells such as hepatocytes. Although liver toxicity of AdCMVtk/GCV has already been described,[13] long-term follow up of the liver lesion has not been previously reported. Here we show that administration of adenovirus containing HSV-tk followed by GCV treatment causes liver damage of diverse intensity. This variability could be due to differences in transduction efficiency or to differences in individual susceptibility to the treatment. In those rats showing severe hepatocellular injury and marked elevation of serum transaminases we observed at weeks 3 and 4 an intense oval cell reaction which was massive at weeks 5 and 6 when hepatocytic differentiation of the oval cells could be detected as nodules of newly formed small hepatocytes near the portal tracts. In contrast, in rats with less intense liver damage and lower serum transaminases oval cell response was slight or absent. These findings suggest that the toxic GCV derivative may cause liver cell damage in a way that division of mature hepatocytes is prevented leading to activation of the stem cell compartment.

There is evidence that liver stem cells reside in bile ducts[20] and, since bile duct cells are not transduced when adenoviral vectors are administered systemically, the facultative stem cells present in the bile ducts might be responsible for the oval cell response when damaged hepatocytes cannot regenerate. However, it is also possible that stem cells are periductular cells[10] which could also be protected from adenoviral infection.

Our data show that after the 7th week some rats developed a nodular regenerative pattern with abundant proliferating ducts surrounding the hepatocellular nodules. This type of lesion would be compatible with a differentiation of oval cells along both hepatocytic and biliary epithelium lineages. Three rats sacrificed at week 8 developed cholangiofibrosis and a cholangiocarcinoma was found in one rat examined at week 36. Cholangiofibrotic lesions showed features of intestinal-like differentiation (intestinal metaplasia) as reflected by the presence of goblet cells and columnar enterocyte-like cells. Similar findings were described by Sirica et al in rats treated with furan where they found increased c-met expression in cholangiofibrotic lesions and in later-developed cholangiocarcinoma.[21–23] In our rats, as in the furan model,[24] the increased expression of c-met in proliferating ductules and in cholangiofibrosis was also associated with features of dysplasia and intestinal metaplasia and with a strong PCNA staining indicating enhanced proliferative activity. These findings suggest a role of c-met in malignant transformation. Expression of c-met was less intense in non-dysplastic proliferating ductules a finding which is compatible with the morphogenetic role of this receptor in particular for structures with lumen formation.[25]

In the model of hepatic stem cell activation here described, as it has also been demonstrated in other models,[26] we show a functional association between HSC and oval cells. In livers showing proliferation of oval cells irradiating from the portal area into the hepatic lobule, desmin positive HSC were observed accompanying the oval cells invading the hepatic lobule, with an apparent parallelism between oval cell proliferation and proliferation of desmin-positive HSC. Similarly HSC strongly expressing α-smooth muscle actin have also been observed surrounding bile ducts in late cholangiofibrotic lesions. Both reactive ductules and HSC[27,28] synthesize TGF-β which stimulates HSC in an autocrine and paracrine manner to produce extracellular matrix (ECM) components. We observed that the presence of HSC was associated with increased deposition of fibronectin and with the presence of collagen and TGF-β around bile ducts in cholangiofibrotic lesions.

The extracellular matrix, in addition to form a physical scaffold for liver cells, is also implicated in important biological functions including differentiation processes and growth regulation.[29,30] HSC besides their role in the production of ECM also express high levels of HGF mRNA.[29] Infusion of HGF has been shown to enhance proliferation not only of oval cells but also of HSC.[19] Our study has shown that HGF mRNA is highly expressed in rats exhibiting either oval cells response or biliary duct hyperplasia but not in those animals with normal liver architecture. In cholangiofibrotic lesions the expression of HGF was detected but at lower levels than in biliary duct hyperplasia without fibrosis suggesting, as proposed by Nakayama et al in a different model of cholangiofibrosis,[31] down-regulation of HGF mRNA by TGF-β. The observed association of HGF mRNA expression with persistent ductular proliferation suggests a role of HGF in the pathogenesis of this lesion possibly by inhibiting ap-

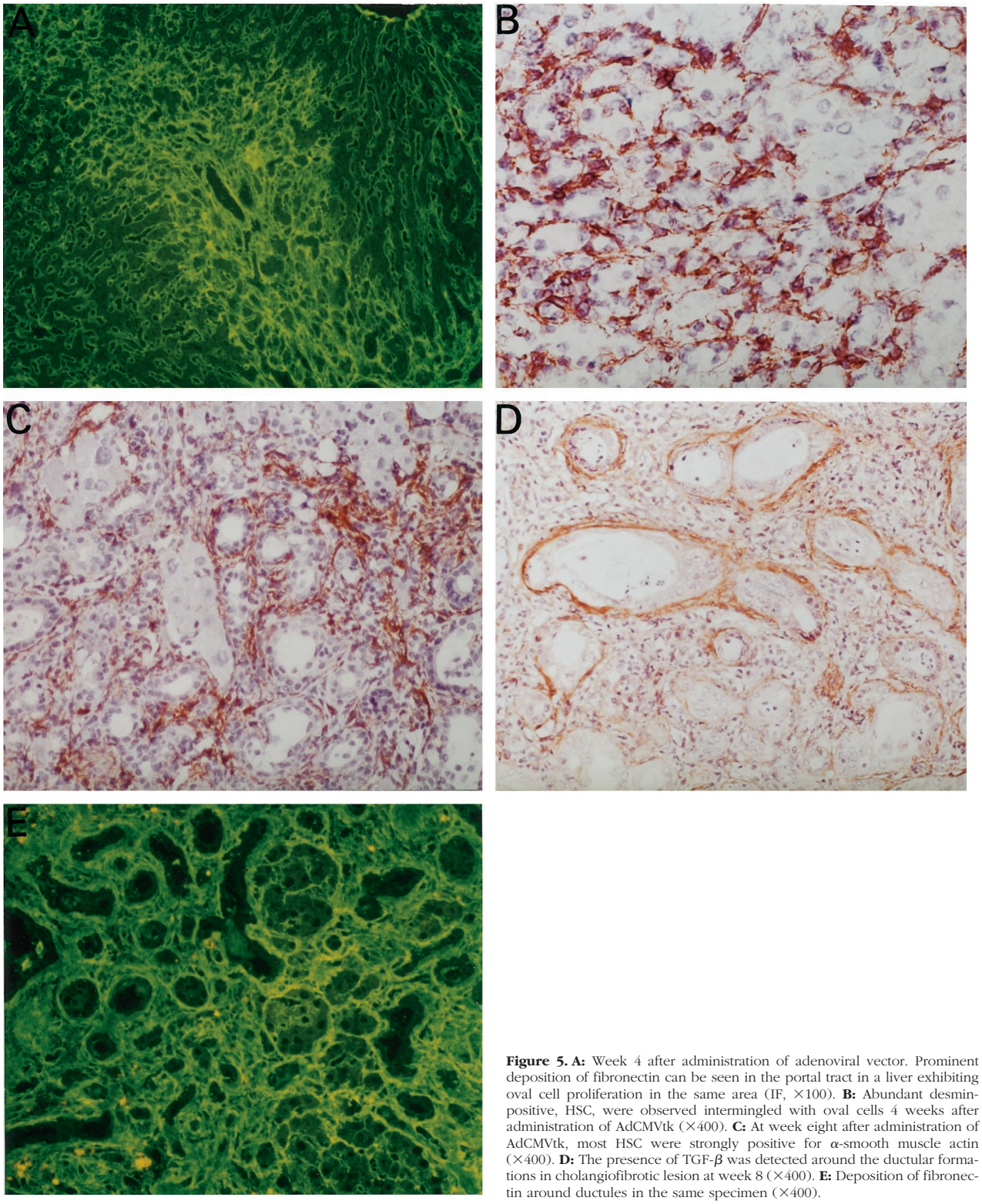

Figure 5. A: Week 4 after administration of adenoviral vector. Prominent deposition of fibronectin can be seen in the portal tract in a liver exhibiting oval cell proliferation in the same area (IF, ×100). **B:** Abundant desmin-positive, HSC, were observed intermingled with oval cells 4 weeks after administration of AdCMVtk (×400). **C:** At week eight after administration of AdCMVtk, most HSC were strongly positive for α-smooth muscle actin (×400). **D:** The presence of TGF-β was detected around the ductular formations in cholangiofibrotic lesion at week 8 (×400). **E:** Deposition of fibronectin around ductules in the same specimen (×400).

optosis of epithelial cells.[32] Seemingly this effect may favor the evolution of ductular proliferation to cholangiocarcinoma as it has been observed in one of our rats 9 months after the administration of the adenoviral vector. Interestingly HGF was detected by immunohistochemistry only in glands with intestinal metaplasia, a lesion which is thought to be associated with the development of cholangiocarcinoma in both humans and experimental animals.[22,24,33] These findings are in agreement with previous reports by Sirica[34] and by Lai et al[35] which showed selective HGF immunoreactivity in intestinal metaplastic glands associated with cholangiofibrosis and in neoplas-

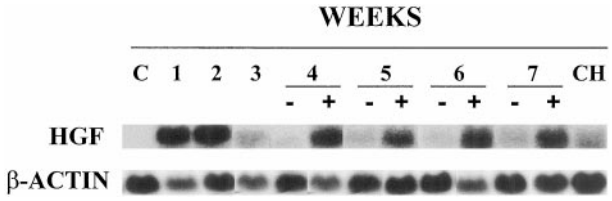

Figure 6. Northern Blot for HGF using total RNA from normal rat liver (C) and in rats treated with AdCMVtk plus ganciclovir 1 to 7 weeks after administration of adenoviral vector. (+) denotes livers with massive oval cell response (weeks 4, 5, and 6) or proliferating bile ducts (week 7). (−) denotes livers with normal architecture at 4, 5, 6, and 7 weeks after treatment. CH is a representative sample corresponding to cholangiofibrosis at week 8. β-actin was used as an internal control.

tic glands of subsequently developed cholangiocarcinoma in the rat furan model.

In summary, we report that the AdCMVtk/GCV system constitutes a new model to stimulate liver regeneration based on a potent oval cell response. This system is simple, does not require partial hepatectomy or the use of carcinogens, and it is especially useful to generate ductular hyperplasia as a source of bile duct epithelium cells. Our results also illustrate the pathological effects in the liver of a type of gene therapy which is being considered as a potential treatment for primary and metastatic liver tumors.

Acknowledgments

We are deeply indebted to Professor Stewart Sell (Albany Medical College, NY) and Dr. Ignacio Melero (University of Navarra, Spain) for helpful suggestions and reviewing the manuscript. We also thank Dr. Douglas Hixson (Brown University, Providence, RI) for the oval cells antibodies and Dr. Jiro Fujimoto (University of Hyogo, Nishinomiya, Japan) for the HGF cDNA.

References

1. Fausto N: Hepatocyte differentiation and liver progenitor cells. Curr Opin Cell Biol 1990, 2:1036–1042
2. Sell S, Pierce GB: Maturation arrest of stem cell differentiation is a common pathway for the cellular origin of teratocarcinomas and epithelial cancers. Lab Invest 1994, 70:6–22
3. Fujio K, Hu Z, Evarts RP, Marsden ER, Niu CH, Thorgeirsson SS: Coexpression of stem cell factor and c-kit in embryonic and adult liver. Exp Cell Res 1996, 224:243–250
4. Evarts RP, Nagy P, Nakatsukasa H, Marsden E, Thorgeirsson SS: In vivo differentiation of rat oval cells into hepatocytes. Cancer Res 1989, 49:1541–1547
5. Factor VM, Radaeva SA, Thorgeirsson SS: Origin and fate of oval cells in dipin-induced hepatocarcinogenesis in the mouse. Am J Pathol 1994, 145:409–422
6. Sirica AE, Gainey TW, Mumaw VR: Ductular hepatocytes. Evidence for a bile ductular cell origin in furan-treated rats. Am J Pathol 1994, 145:375–383
7. Lemire JM, Shiojiri N, Fausto N: Oval cell proliferation and the origin of small hepatocytes in liver injury induced by D-galactosamine. Am J Pathol 1991, 139:535–552
8. Yasui O, Miura N, Terada K, Kawarada Y, Koyama K, Sugiyama T: Isolation of oval cells from Long-Evans Cinnamon rats and their transformation into hepatocytes in vivo in the rat liver. Hepatology 1997, 25:329–334
9. Wu H, Wade M, Krall L, Grisham J, Xiong Y, Van Dyke T: Targeted in vivo expression of the cyclin dependent kinase inhibitor p21 halts hepatocyte cell cycle progression, postnatal liver development, and regeneration. Genes Dev 1996, 10:245–260
10. Sell S: Is there a liver stem cells? Cancer Res 1990, 50:3811–3815
11. Qian C, Bilbao R, Bruña O, Prieto J: Induction of sensitivity to ganciclovir in human hepatocellular carcinoma cells by adenovirus-mediated gene transfer of herpes simplex virus thymidine kinase. Hepatology 1995, 22:118–123
12. Qian C, Idoate M, Bilbao R, Sangro B, Bruna O, Vazquez J, Prieto J: Gene transfer and therapy with adenoviral vector in rats with diethylnitrosamine-induced hepatocellular carcinoma. Hum Gene Ther 1997, 8:349–358
13. van der Eb MM, Cramer SJ, Vergouwe Y, Schagen FH, van Krieken JH, van der Eb AJ, Rinkes IH, van de Velde CJ, Hoeben RC: Severe hepatic dysfunction after adenovirus-mediated transfer of the herpes simplex virus thymidine kinase gene and ganciclovir administration. Gene Ther 1998, 5:451–458
14. Wachstein M, Meisel E: On the histochemical demonstration of glucose-6-phosphatase. J Histochem Cytochem 1956, 4:592
15. Chomczynski P: A reagent for the single-step simultaneous isolation of RNA, DNA and proteins from cell and tissue samples. BioTechniques 1993, 15:532–535
16. Yang L, Faris RA, Hixson DC: Phenotypic heterogeneity within clonogenic ductal cell populations isolated from normal adult rat liver. Proc Soc Exp Biol Med 1993, 204, 280–288
17. Yang L, Faris RA, Hixson DC: Characterization of a mature bile duct antigen expressed on a subpopulation of biliary ductular cells but absent from oval cells. Hepatology 1993, 18:357–366
18. Alison MR, Poulsom R, Jeffery R, Anilkumar TV, Jagoe R, Sarraf CE: Expression of hepatocyte growth factor mRNA during oval cell activation in the rat liver. J Pathol 1993, 171:291–309
19. Nagy P, Bisgaard HC, Santoni-Rugiu E, Thorgeirsson S: In vivo infusion of growth factors enhances the mitogenic response of rat hepatic ductal (oval) cells after administration of 2-acetaminofluorene. Hepatology 1996, 23:71–79
20. Novikoff PM, Yam A, Oikawa I: Blast-like cell compartment in carcinogen-induced proliferating bile ductules. Am J Pathol 1996, 148: 1473–1492
21. Elmore LW, Sirica EA: Phenotypic characterization of metaplastic intestinal glands and ductular hepatocytes in cholangiofibrotic lesions rapidly induced in the caudate liver lobe of rats treated with furan. Cancer Res 1991, 51:5752–5759
22. Elmore LW, Sirica AE: ''Intestinal-type'' of adenocarcinoma preferentially induced in right/caudate liver lobes of rats treated with furan. Cancer Res 1993, 53:254–259
23. Sirica AE, Cole SL, Williams T: A unique rat model of bile ductular hyperplasia in which liver is almost totally replaced with well-differentiated bile ductules. Am J Pathol 1994, 144:1257–1268
24. Radaeva S, Ferreira-Gonzalez A, Sirica AE: Overexpression of C-NEU and C-MET during rat liver cholangiocarcinogenesis: a link between biliary intestinal metaplasia and mucin-producing cholangiocarcinoma. Hepatology 1999, 29:1453–1462
25. Tsarfaty I, Resau JH, Rulong S, Keydar I, Faletto DL, Vande Woude GF: The met proto-oncogene receptor and lumen formation. Science 1992, 257:1258–1261
26. Vetsuka K, Suzuki M, Nakayama H, Doi K: Prolonged oval cell proliferation with Ito cell activation and extracellular matrix accumulation in galactosamine-induced acute hepatitis in mini rats. Histol Histopathol 1997, 12:937–943
27. Milani S, Herbst H, Schuppan D, Stein H, Surrenti C: Transforming growth factors beta 1 and beta 2 are differentially expressed in fibrotic liver disease. Am J Pathol 1991, 139:1221–1229
28. Nagy P, Evarts RP, McMahon JB, Thorgeirsson SS: Role of TGF-beta in normal differentiation and oncogenesis in rat liver. Mol Carcinog 1989, 2:345–354
29. Martinez-Hernandez A, Martinez DF, Amenta PS: The extracellular matrix in hepatic regeneration: localization of collagen types I, III, IV, laminin and fibronectin. Lab Invest 1991, 64:157–166
30. Saile B, Matthes N, Knittel T, Ramadori G: Transforming growth factor β and tumor necrosis factor α inhibit both apoptosis and proliferation of activated rat hepatic stellate cells. Hepatology 1999, 30:196–202

31. Nakayama N, Kashiwazaki H, Kobayashi N, Hamada J-I, Ogiso Y, Itakura Y, Matsumoto K, Nakamura T, Koike T, Kuzumaki N, Takeichi N: Hepatocyte growth factor and c-met expression in Long-Evans Cinnamon rats with spontaneous hepatitis and hepatoma. Hepatology 1996, 24:596–602
32. Yo Y, Morishita R, Nakamura S, Tomita N, Yamamoto K, Moriguchi A, Matsumoto K, Nakamura T, Higaki J, Ogihara T: Potential role of hepatocyte growth factor in the maintenance of renal structure: anti-apoptotic action of HGF on epithelial cells. Kidney Int 1998, 54:1228–1238
33. Kozuka S, Kurashina M, Tsubone M, Hachisuka K, Yasui A: Significance of intestinal metaplasia for the evolution of cancer in the biliary tract. Cancer 1984, 54:2277–2285
34. Sirica AE: Biliary proliferation and adaptation in furan-induced rat liver injury and carcinogenesis. Toxicol Pathol 1996, 24:90–99
35. Lai G-H, Radaeva S, Nakamura T, Sirica AE: Unique epithelial cell production of hepatocyte growth factor/scatter factor by putative precancerous intestinal metaplasias and associated ''intestinal-type'' biliary cancer chemically-induced in rat liver. Hepatology 2000, 31:1257–1265